Demagnetization curves at different temperatures for single-phase nanocrystalline Nd-Fe-B magnets studied micromagnetically

2001 J. Phys.: Condens. Matter 13 3865

(http://iopscience.iop.org/0953-8984/13/17/307)

INSTITUTE OF PHYSICS PUBLISHING JOURNAL OF PHYSICS: CONDENSED MATTER

J. Phys.: Condens. Matter **13** (2001) 3865–3874 www.iop.org/Journals/cm PII: S0953-8984(01)16167-9

Demagnetization curves at different temperatures for single-phase nanocrystalline Nd–Fe–B magnets studied micromagnetically

Zhao Sufen, Jin Hanmin, Wang Xuefeng and Yan Yu

Department of Physics, Jilin University, Changchun, 130023, People's Republic of China

Received 7 August 2000, in final form 15 March 2001

Abstract

The demagnetization curves at different temperatures between 4 and 250 K were calculated for single-phase nanocrystalline Nd–Fe–B magnets by using the micromagnetic finite-element technique. The calculations were carried out for a model magnet comprised of 216 grains of dimension 20 nm, taking into account the anisotropic characteristics of the curve with respect to the field direction. The calculations simulate the experimental curves for the nanocrystalline $Nd_{13}Fe_{77}B_{10}$ magnet fairly well. The inter-grain exchange interaction in the magnet is estimated to be about 75% of the intra-grain exchange interaction.

1. Introduction

Rapidly quenched nanocrystalline Nd–Fe–B magnets are isotropic. Since 1996, many calculations have been performed on the demagnetization curves for such magnets by using the micromagnetic finite-element technique, mostly by the group of Fischer, Schrefl, Kronmüller, and Fidler [1]. The quality of the calculations, however, is not good. For example, ${}_iH_c$ as a function of the grain size L calculated for the stoichiometric composition takes values larger than the experimental values for the Nd-rich $Nd_{2.33}Fe_{14}B_{1.06}Si_{0.21}$ magnets [2] by 60–170% [1], while they should be smaller. Since the inter-grain exchange interaction for the magnet of stoichiometric composition with $Nd_2Fe_{14}B$ grains in direct contact is larger than that of Nd-rich magnets with a Nd-rich paramagnetic boundary phase separating the grains, ${}_iH_c$ for the former should be smaller than that for the latter. Griffiths *et al* [3] simulated the ${}_iH_c \sim L$ relation much better by using a grain number N larger than that (namely 35) used in [1].

Recently, it was found that the calculated demagnetization curves, especially that for ${}_iH_c$, strongly depend on the applied field direction [4, 5]. The difference between the values of ${}_iH_c$ along different field directions can reach as much as $\sim$0.8 MA m^{-1} for a system with grain number $N = 30$–60. The range of the difference and the average of ${}_iH_c$ decrease with increase of N [4, 6]. With increase of N to infinity, the range should decrease to zero and ${}_iH_c$ should approach the limit ${}_iH_c(N \to \infty)$. ${}_iH_c(N \to \infty)$ can be obtained by extrapolation. Figure 1 [6] demonstrates the $J_r/J_s \sim n$ and $\mu_0\,{}_iH_c \sim n$ relations at room temperature for the

0953-8984/01/173865+10$30.00

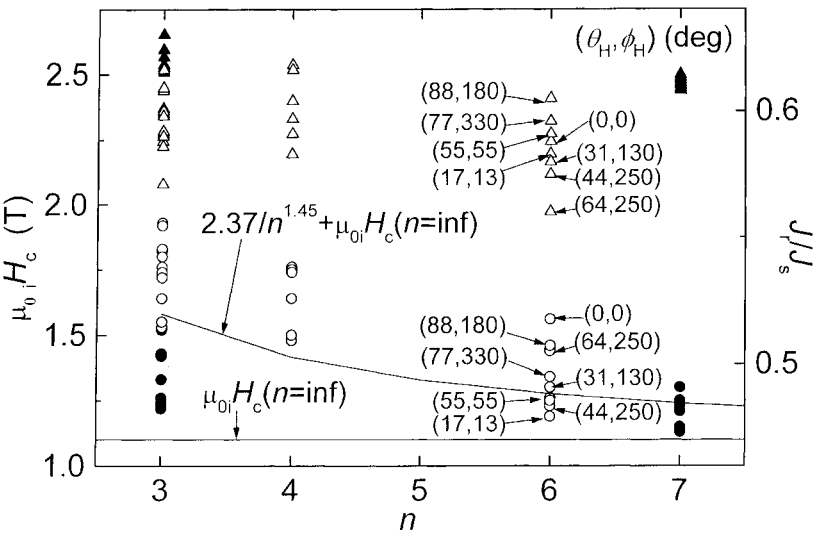

Figure 1. J_r/J_s (triangles) and ${}_i H_c$ (circles) calculated along different field directions for $L = 20$ nm and $n = 3$, 4, 6 and 7 [6]. The different symbols for a given n are the values calculated along different field directions. The open symbols are for the present model (model G) with the dimension of the element ∼1.4 nm, and the full symbols for model S with element dimension ∼1.7 nm.

stoichiometric composition magnets with $L = 20$ nm. Here, $n = N^{1/3}$ is the grain number along the edge of the cubic magnet. The different symbols for a given n are the values calculated along different field directions (θ_H, ϕ_H) . The open circles (model G) were calculated using this paper's model (see the next paragraph), and the full circles (model S) using another model in which each grain is divided into tetragonal elements and the direction of $\vec{J}_s$ varies linearly within each element. The latter presents a smaller range and an average of $\mu_{0\,i}H_c(n)$, and the average decreases more smoothly with increase of n. The $\mu_{0\,i}H_c \sim n$ data for different L have been fitted by the relation $\mu_{0\,i}H_c(n) = C/n^t + \mu_{0\,i}H_c(n = \infty)$ in which C, t and $\mu_{0\,i}H_c(n = \infty)$ are fitting parameters. It was found that $\mu_{0\,i}H_c$ calculated for finite n is larger than or equal to $\mu_{0\,i}H_c(n = \infty)$. Apparently the curve calculated along an arbitrarily selected field direction for a small-N system has only qualitative meaning. For quantitative analyses the limit curve corresponding to $N \to \infty$ should be obtained. For this purpose a number of curves for several values of n and field directions should be calculated in advance. A fairly reliable value of $\mu_{0\,i}H_c(n = \infty)$ could be obtained for smaller L, such as for $L = 4.4$ nm for which the maximum of n used for the calculation, n_{max}, is as large as 20 ($N = 8000$). Such an approach, however, is too time consuming, and becomes less reliable for larger L for which the n_{max} that we can treat becomes smaller ($n_{max} \propto 1/L$ for a given CPU (central processing unit) time). Another approach, especially convenient for large L, is to calculate several curves along different field directions for a large n and select the curve which has the smallest $\mu_{0\,i}H_c$ as the best approximation to the limit curve for $N = \infty$ among the curves. By taking such approaches, the $J_r/J_s \sim L$ and ${}_i H_c \sim L$ relations for the $Nd_{2.33}Fe_{14}B_{1.06}Si_{0.21}$ magnet could be simulated well by the calculations for the magnets of stoichiometric composition. The values of J_r/J_s are larger by ∼0.05 and those of ${}_i H_c$ are the same as or somewhat smaller than the experimental values, which is reasonable [4, 6].

The anisotropic characteristic of the curve for finite N is expected from the discrete distribution of the N c-axes distributed nearly uniformly over the whole 4π solid-angle space.

In the case of $N \approx 30$, for instance, the c-axis makes an angle of around 30° with the neighbouring c-axes in the solid-angle space. The change of the field direction causes the change of the angles of the field direction with the c-axes, which affects the demagnetization process causing the change in the demagnetization curve. With increase of N to infinity, the angle between the neighbouring c-axes in the solid-angle space decreases to zero, causing the decrease of the anisotropy to zero. It is striking, however, that for the curve calculated using the Stoner–Wohlfarth (S–W) model in which the grains are considered as isolated single domains without interactions between them, the anisotropy is negligibly small and a system of $N \gtrsim 30$ can be considered essentially isotropic. The curve is not only isotropic but also independent of N ($N \gtrsim 30$) [4, 6]. The results show that the inter-grain exchange interaction bringing the demagnetization processes of the grains into a unified non-coherent rotation is also a key factor contributing to the anisotropic characteristic of the curve.

The demagnetization curves at different temperatures for the Nd–Fe–B magnets have been studied by some of this paper's authors in cooperation with other workers [7, 8]. The calculations have two shortcomings. The first is that the curves were calculated along an arbitrarily selected field direction for a system with N as small as 27. As is pointed out above, such an approach is inadequate for quantitative analyses. The second is that the intra-grain exchange interaction parameter was treated as a fitting parameter while the exchange constant A for $Nd_2Fe_{14}B$ is known from experiment. This paper will study again the curves at different temperatures, taking into account the anisotropic characteristics of the curves and exploiting the experimental value of A.

2. Models and calculations

The model magnet is the same as that of Griffiths *et al* [3], and is composed of $N = n \times n \times n$ cubic $Nd_2Fe_{14}B$ grains of size L. The directions of the c-axes of the grains $(\theta_c(i), \varphi_c(i))$ $(i = 1, 2, \ldots, N)$ are distributed nearly uniformly in the 4π solid-angle space by taking the values of θ_c from 0 to 90° in appropriate steps $\Delta\theta_c$ and dividing each circumference around the $\theta_c = 0$ axis for a given θ_c, $2\pi \sin\theta_c$, by an integer to make the relation $\sin\theta_c \, \Delta\varphi_c \approx \Delta\theta_c$ hold. The c-axes are assigned to the grains randomly to simulate the isotropy of the real magnets. Each grain is divided into $m \times m \times m$ single-domain elements of dimension L/m. Each element is exchange coupled with the six adjacent elements. The infinite magnet is built up by piling up the finite magnets periodically so that the periodic boundary conditions of the magnetic properties hold for the finite magnet. The energy for the magnet consists of the exchange interaction F_{ex}, the magnetocrystalline anisotropy energy F_K and the Zeeman energy F_H. The stray-field energy which plays a minor role [8] but consumes a much larger CPU time was neglected. The intra-grain exchange interaction, for instance between the elements (i, j, k) and $(i + 1, j, k)$ $(i, j, k = 1, 2, \ldots, nm)$, within a grain was approximated by

$$\begin{aligned} F_{ex}(i, j, k; i+1, j, k) &= \left(\frac{L}{m}\right)^2 \int_i^{i+1} A[(\nabla\alpha_x)^2 + (\nabla\alpha_y)^2 + (\nabla\alpha_z)^2] \, \mathrm{d}x \\ &\approx \left(\frac{L}{m}\right)^2 A \sum_{\gamma=x,y,z} \left[\frac{\alpha_\gamma(i+1, j, k) - \alpha_\gamma(i, j, k)}{L/m}\right]^2 \frac{L}{m} \\ &= \frac{2LA}{m}\left[1 - \frac{\vec{J}_s(i, j, k) \cdot \vec{J}_s(i+1, j, k)}{J_s^2}\right] \end{aligned}$$

where α_γ $(\gamma = x, y, z)$ are the direction cosines of the magnetic polarization vector $\vec{J}_s$. When the two elements belong to different grains, the exchange interaction between them should be

smaller than the intra-grain exchange interaction for a Nd-rich magnet in which the grains are separated by a grain boundary layer. The inter-grain exchange interaction is also described by the above relation but with the exchange constant A replaced by βA ($0 \leqslant \beta \leqslant 1$). $F_K + F_H$ is simply the sum of the energies of the elements:

$$F_K + F_H = \left(\frac{L}{m}\right)^3 \sum_{i,j,k=1}^{nm} [K_1 \sin^2\theta_{\langle 100\rangle}(i,j,k) + K_2 \sin^4\theta_{\langle 100\rangle}(i,j,k) + K_3 \sin^4\theta_{\langle 100\rangle}(i,j,k)\cos(4\varphi_{\langle 100\rangle}(i,j,k)) - \vec{J}_s(i,j,k)\cdot\vec{H}]$$

where $\theta_{\langle 100\rangle}$ is the angle between $\vec{J}_s$ and the c-axis. The value of A is 7.7×10^{-12} J m^{-1} at room temperature [1] and is assumed to vary with temperature in proportion to $J_s(T)^2$ according to the molecular-field approximation. The values of $J_s(T)$ from [9], and the values of $K_1(T)$, $K_2(T)$ and $K_3(T)$ from [10], all measured for bulk single crystals, are listed in table 1. Since $\mu_0 {}_i H_c$ for $L = 20$ nm is smallest along the field direction $(\theta_H, \phi_H) = (17^\circ, 13^\circ)$ for $n = 6$ ($N = 216$) and $m = 14$ ($L/m \approx 1.4$ nm $\approx$ one third of the domain wall thickness) in figure 1, the curves at different temperatures were calculated along this field direction for the same n, L, m and $\beta \neq 0$. The calculations were also carried out for $N = \infty$, $m = 1$ and $\beta = 0$ (the S–W model) for reference.

Table 1. The values of $J_s(T)$ [9] and $K_1(T)$, $K_2(T)$ and $K_3(T)$ [10].

T (K)	J_s [9] (T)	K_1 [10] (10^6 J m^{-3})	K_2 [10] (10^6 J m^{-3})	K_3 [10] (10^6 J m^{-3})
4	1.86	−16	27	0.45
40	1.86	−14	26	0.38
100	1.86	−8	21	0.24
125	1.85	−4.4	17	0.1
145	1.79	0	13	0
150	1.78	1.8*	11*	0
180	1.76	4	4.7	0
250	1.70	6	1	0

* The values in [8] were misprinted.

The applied field was decreased from 4 MA m^{-1} in steps, and the polarization J at each field was obtained from minimization of the energy with respect to the polar angles of $\vec{J}_s$ for the elements $\{\theta(i,j,k), \phi(i,j,k)\}$ $(i,j,k = 1, 2, \ldots, nm)$. The minimization of the energy was achieved by using the conjugate gradient method [11]. The curves were compared with the experimental curves for the nanocrystalline $Nd_{13}Fe_{77}B_{10}$ magnet [7, 8].

3. Results and discussion

Figure 2 shows the temperature dependence of $J(H = 4$ MA m$^{-1})$. It can be seen that 0.85 times the calculated values coincides with the experimental values, showing that the non-magnetic grain boundary phases hold about 15% of the volume of the $Nd_{13}Fe_{77}B_{10}$ magnet. Hereafter, the calculated J-values for the curves are multiplied by 0.85.

Figures 3(a) to 3(g) display the demagnetization curves at 4.2 K, 40 K, 100 K, 125 K, 150 K, 180 K and 250 K, respectively, calculated for $\beta = 1$ and 0.75 along with the experimental curves. The results for $\beta = 1$ and 0.75 are essentially the same in the first quarter. In the second quarter, $J(H)$ for $\beta = 0.75$ is smaller than that for $\beta = 1$ below about the spin-reorientation

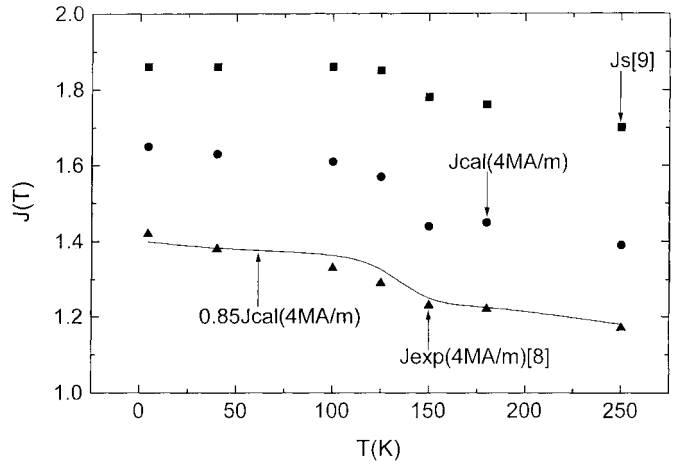

Figure 2. The temperature dependence of $J(H = 4\ \mathrm{MA\ m^{-1}})$ and J_s.

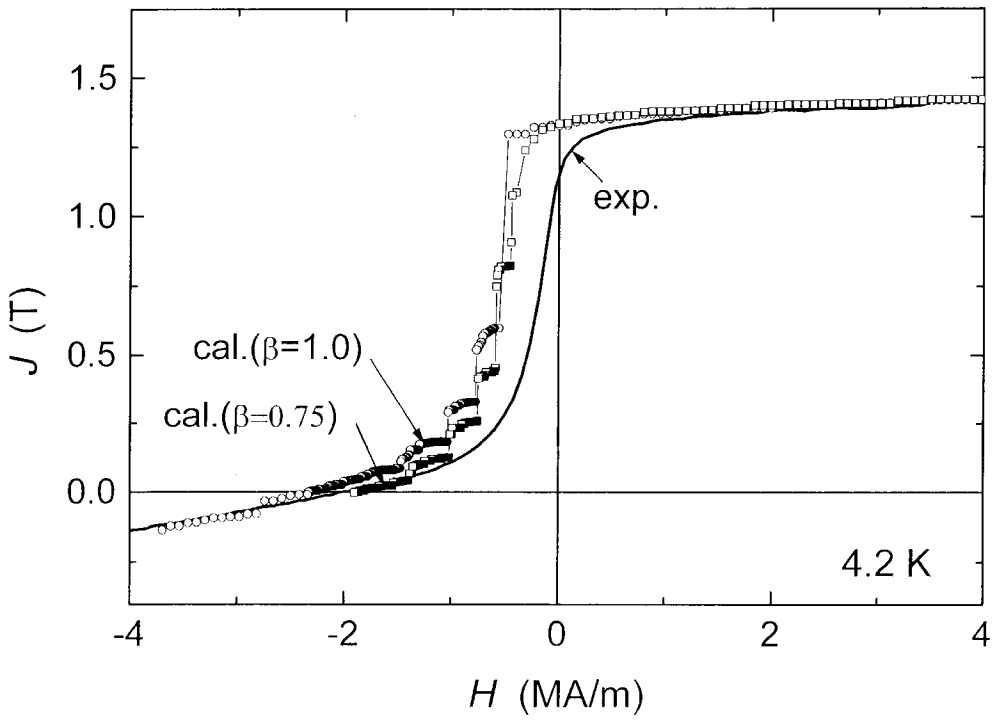

(a)

Figure 3. The damagnetization curves at 4.2 K (a), 40 K (b), 100 K (c), 125 K (d), 150 K (e), 180 K (f) and 250 K (g). Symbols + line: calculation. Line: experiment [8].

temperature $T_s = 135$ K, and becomes larger above $\sim T_s$. The results for $\beta = 0.75$ simulate the experimental results fairly well. However, the values of J are apparently larger than the experimental values in the second quarter where the curve descends steeply. The inconsistency is striking below T_s.

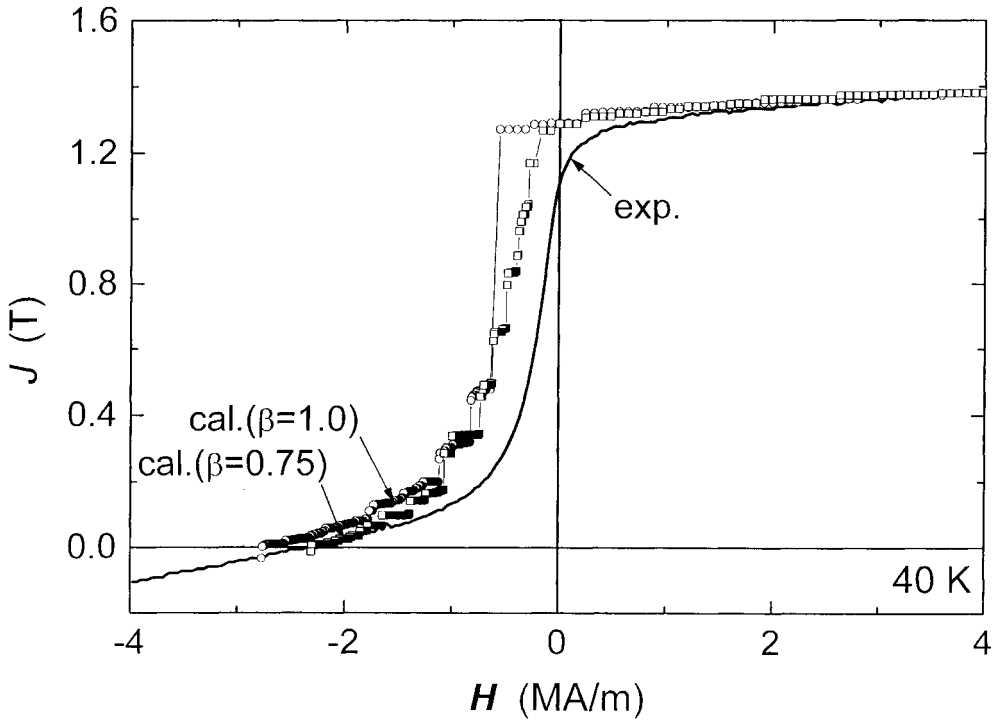

(b)

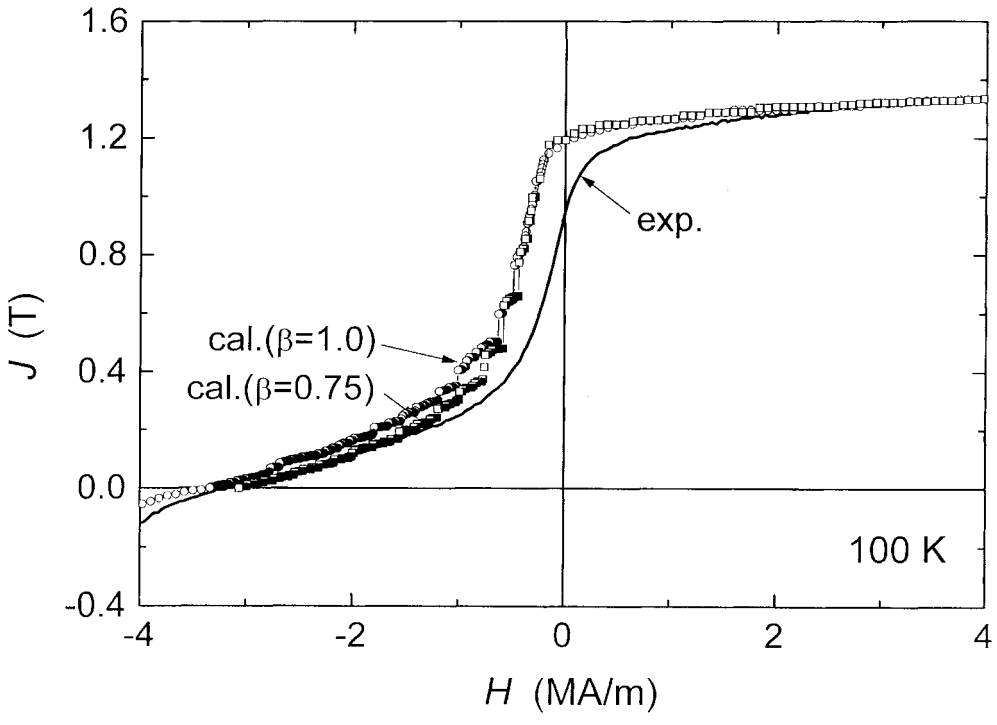

(c)

Figure 3. (Continued)

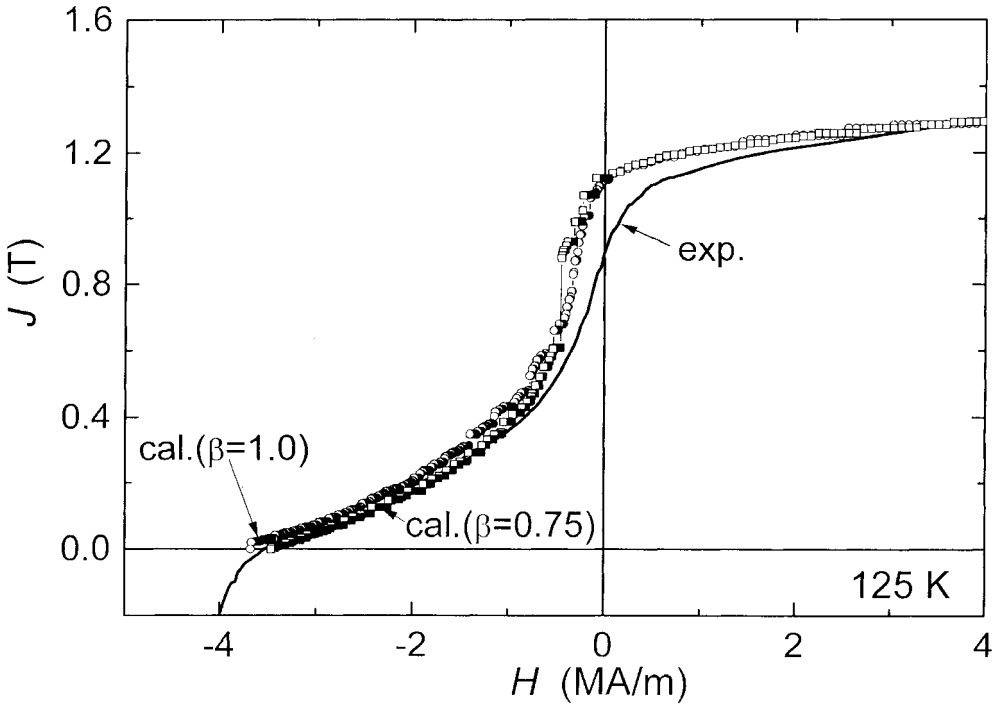

(d)

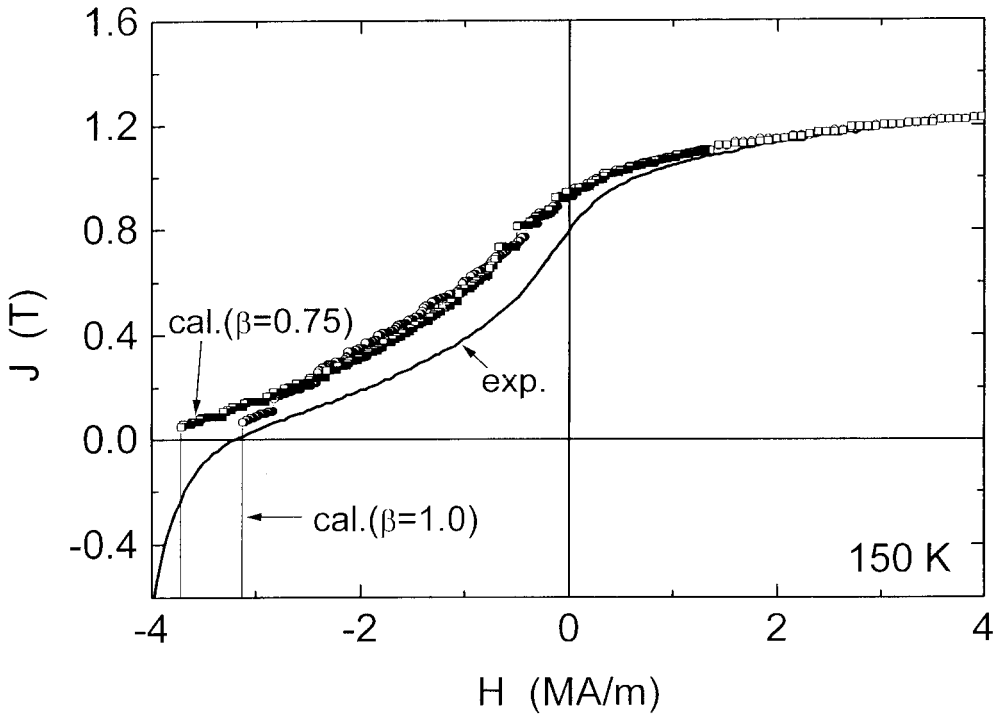

(e)

Figure 3. (Continued)

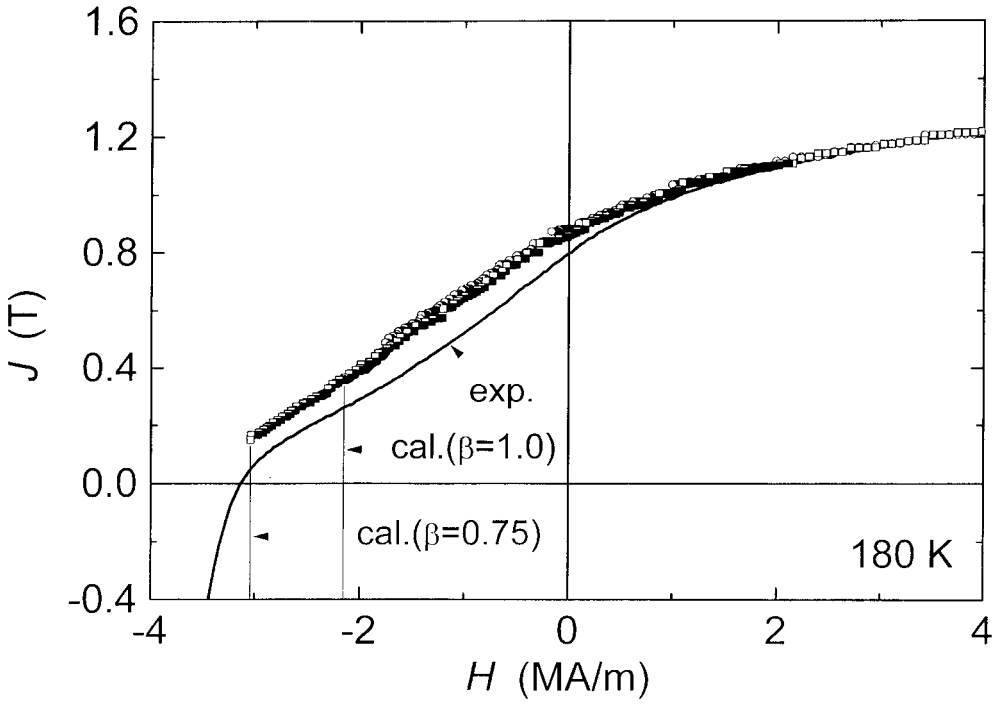

(f)

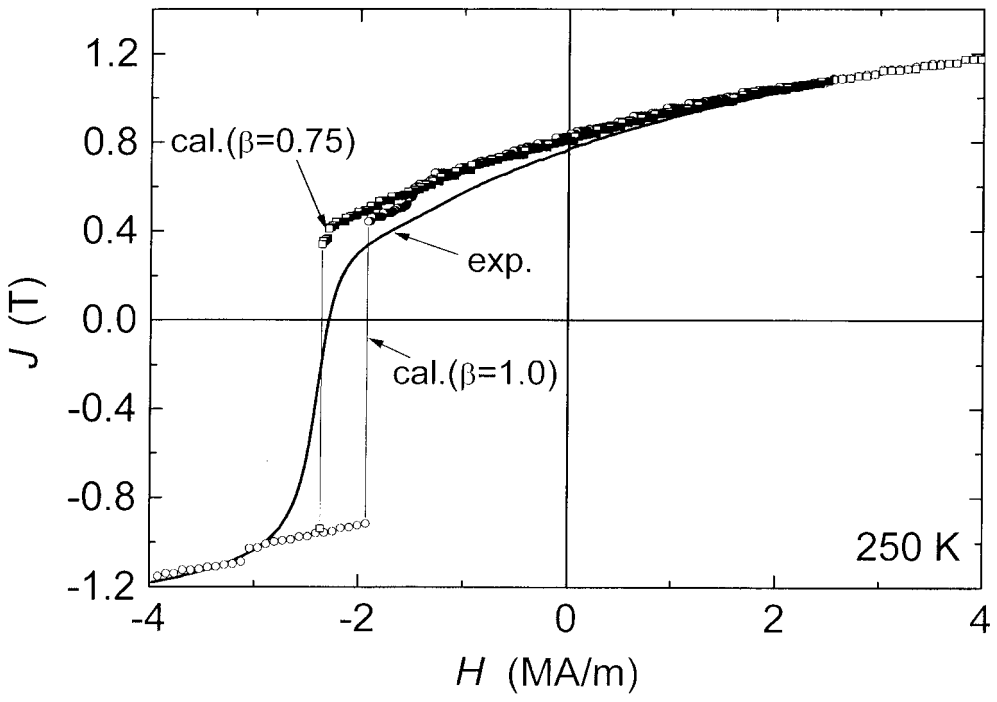

(g)

Figure 3. (Continued)

Figure 4 shows the temperature dependence of ${}_iH_c$. The calculations are for $\beta = 1.0$, 0.75, 0.6 and 0. With increase of temperature, ${}_iH_c$ increases, reaches a maximum around T_s and then decreases for all β in accordance with the experimental result [8]. With increase of β, ${}_iH_c$ increases in the temperature range below $\sim T_s$, but decreases in the temperature range above $\sim T_s$. So the curves for $\beta = 1$ and 0 (S–W model) represent the theoretical upper and lower limits below $\sim T_s$, and the lower and upper limits above $\sim T_s$, respectively. The experimental results are within the same range, and the coincidence of the calculations for $\beta = 0.75$ with the experimental results is excellent. Though apparent inconsistency is observed at 150 K, the calculated ${}_iH_c$ correctly corresponds to the steepest part of the experimental curve where the irreversible demagnetization is proceeding (figure 3(e)). The difference in behaviour of the ${}_iH_c \sim T$ relation below and above $\sim T_s$ is related to the different kinds of magnetocrystalline anisotropy of $Nd_2Fe_{14}B$. $Nd_2Fe_{14}B$ has an axial anisotropy with the easy axis along the c-axis above T_s and an easy-cone anisotropy with four easy axes tilted from the c-axis toward the c-plane in the {110} planes. The cone angle θ_c ($\sin\theta_c \approx -K_1/2K_2$) increases from zero to about 33° when temperature decreases from T_s to 0 K. The irreversible demagnetization process above T_s is the irreversible rotation from around the positive directions of the c-axes toward the negative directions of the c-axes. Below T_s, since the in-plane energy barrier $2K_3\sin^4\theta_c \approx K_3K_1^2/2K_2^2$ is smaller than the axial energy barrier $\sim K_1(1-\sin^2\theta_c)+K_2(1-\sin^4\theta_c)$ by more than two orders of magnitude, $\vec{J}_s$ irreversibly rotates around the cone, first causing the first step in the demagnetization curve between $H = 0$ and $H = -{}_iH_c$, after which another irreversible rotation towards the opposite direction of the cone occurs causing the second step [7].

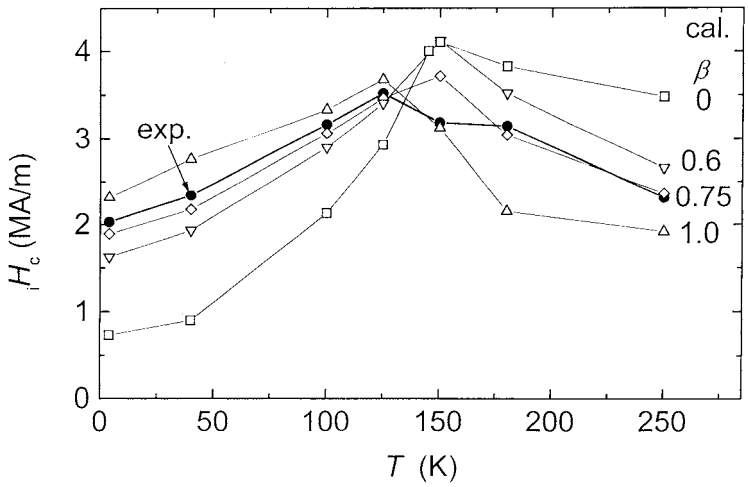

Figure 4. The temperature dependence of ${}_iH_c$. Open symbols + line: calculation. Full symbols + line: experiment [8].

Figure 5 shows the temperature dependence of the normal remanence J_r/J_s. J_r/J_s decreases with increase of temperature monotonically. With increase of β from 0 to 1, J_r/J_s increases, but the increase is very limited below $\sim T_s$. It is noticeable that below T_s the experimental values of J_r/J_s are apparently smaller than the theoretical lower limits given by the S–W model. This seemingly unreasonable result could be caused by neglect of the stray field. Since the in-plane energy barrier between the easy axes is fairly small, the magnetic stray field can affect the demagnetization process, causing a large decrease in J.

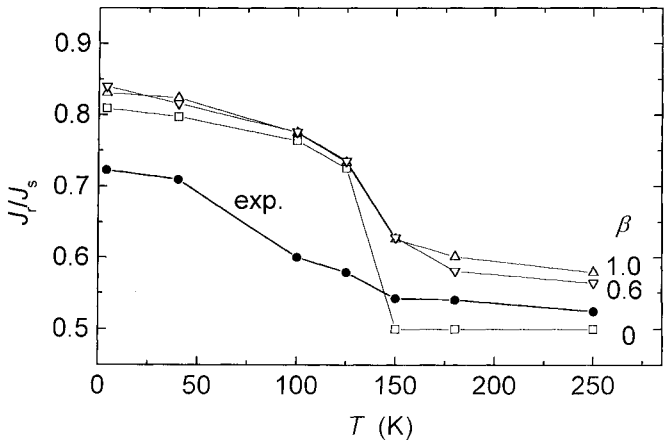

Figure 5. The temperature dependence of J_r/J_s. Open symbols + line: calculation. Full symbols + line: experiment [8].

In summary, taking into account the anisotropic characteristics of the demagnetization curve, the demagnetization curves at different temperatures for the $Nd_{13}Fe_{77}B_{10}$ magnet [8] are simulated fairly well by micromagnetic calculations. The inter-grain exchange interaction for the $Nd_{13}Fe_{77}B_{10}$ magnet is estimated to be about 75% of the intra-grain exchange interaction.

Acknowledgment

This work was supported by the National Science Foundation of China.

References

[1] Fischer R, Schrefl T, Kronmüller H and Fidler J 1996 *J. Magn. Magn. Mater.* **153** 35
[2] Manaf A, Buckley R A, Davies H A and Leonowicz M 1991 *J. Magn. Magn. Mater.* **101** 360
[3] Griffiths M K, Bishop J E L, Tucker J W and Davies H A 1998 *J. Magn. Magn. Mater.* **183** 49
[4] Jin H M, Zhao S F, Wang X F and Yan Y 1999 *Proc. 1st Int. Symp. on Magnetic Materials and Applications (Taejon, Korea)* p 67
[5] Jin H M, Zhao S F and Wang X F 2000 *J. Mater. Sci. Technol.* **16** 107
[6] Jin H M, Wang X F, Zhao S F and Yan Y 2001 *Chinese Phys.* at press
[7] Jin H M, Kim Y B, Park W S, Park M J and Wang X F 1998 *J. Phys.: Condens. Matter* **10** 389
[8] Jin H M, Kim Y B and Wang X F 1998 *J. Phys.: Condens. Matter* **10** 7243
[9] Hirosawa S, Matsuura Y, Yamamoto H, Fujimura S, Sagawa M and Yamauchi M 1986 *J. Appl. Phys.* **59** 873
[10] Sagawa M, Hirosawa S, Yamamoto H, Fujimura S and Matsuura Y 1987 *Japan. J. Appl. Phys.* **26** 785
[11] Murray W and Wright M H 1981 *Practical Optimization* (London: Academic)